AD NUMBER

AD835043

NEW LIMITATION CHANGE

TO

Approved for public release, distribution unlimited

FROM

Distribution authorized to U.S. Gov't. agencies and their contractors; Critical Technology; MAY 1968. Other requests shall be referred to Naval Weapons Center, China Lake, CA 93555.

AUTHORITY

Naval Weapons Center ltr dtd 24 Mar 1972

NWC TP 4544

AN ANALYSIS OF AXIAL ACOUSTIC WAVES IN A COLD-FLOW ROCKET

by

F. E. C. Culick
and
G. L. Dehority

Research Department

ABSTRACT. The presence of waves in a rocket chamber depends on the relative importance of energy supplied by interaction with the combustion processes and energy lost through dissipative processes. As an aid to assessing the latter, the cold-flow rocket appears to be a promising tool for both research and development. Combustion is absent and acoustic waves are excited mechanically in a chamber through which a steady flow is maintained. The analysis presented here is intended to serve as a basis for interpreting such measurements. Only the case of axial, or longitudinal waves is treated, and results show mainly how the losses at the exhaust end of the chamber may be inferred from measurements of the transient response and the frequency response of a chamber.

NAVAL WEAPONS CENTER
CHINA LAKE, CALIFORNIA * MAY 1968

DISCLAIMER NOTICE

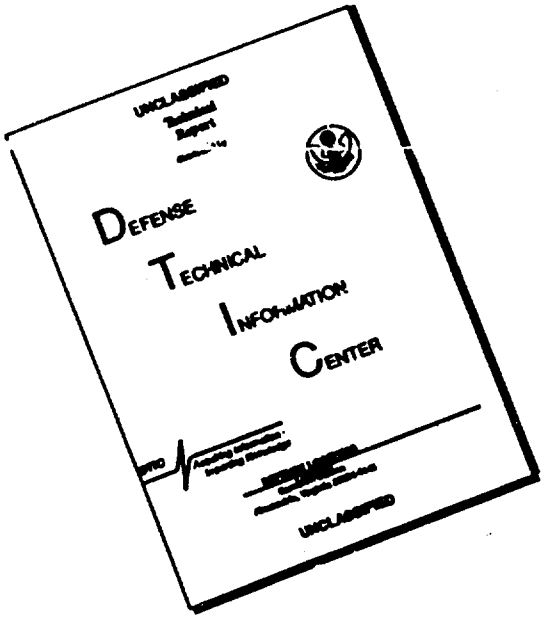

THIS DOCUMENT IS BEST QUALITY AVAILABLE. THE COPY FURNISHED TO DTIC CONTAINED A SIGNIFICANT NUMBER OF PAGES WHICH DO NOT REPRODUCE LEGIBLY.

NAVAL WEAPONS CENTER
AN ACTIVITY OF THE NAVAL MATERIAL COMMAND

M. R. Etheridge, Capt., USN ..... Commander
Thomas S. Amlie, Ph.D. ..... Technical Director

FOREWORD

This report presents the results of an analytical study of one-dimensional wave behavior in channels terminated by a nozzle. The effect of the nozzle on the flow field is given in terms of this acoustic admittance at the nozzle entrance. A comparison is made of the behavior of freely decaying waves and of steady-state waves driven at the head end of the channel.

The material in the report should be helpful in the planning of cold-flow experiments to determine acoustic damping constants. It should also aid in the correlation and interpretation of the experimental results of such tests.

This work was carried out under Naval Ordnance Systems Command Task Assignment ORD-033 103/200 1/F009-06-01, PA #3.

This report is transmitted for information only. It does not represent the official views or final judgment of this Center.

Released by
J. E. CRUMP, Acting Head
Aerothermochemistry Division
9 April 1968

Under authority of
HUGH W. HUNTER, Head
Research Department

NWC Technical Publication 4544

Published by.....Research Department
Collation.....Cover, 18 leaves, DD Form 1473, abstract cards
First printing.....225 unnumbered copies
Security classification.....UNCLASSIFIED

TABLE OF CONTENTS

Figures:

NOMENCLATURE

A	Admittance at boundary, defined by Eq. 9
a	Sonic velocity, also "effective" plane where mean chamber conditions are reached (Fig. 1)
b	"Effective" plane of nozzle entrance (Fig. 1)
c_p	Specific heat at constant pressure
D	Dimensionless expression defined by Eq. 35
$\hat{e}_z$	Unit axial vector
f	Dimensional frequency; also "non-homogeneous" part of pressure boundary equation (Eq. 8)
h	"Non-homogeneous" part of pressure wave equation (Eq. 7)
k	Non-dimensional wave number for steady oscillations $\frac{\omega L}{a}$
k_ℓ	Non-dimensional wave number for purely axial mode oscillations
k_N	Non-dimensional wave number for classical mode oscillations
L	Chamber length
ℓ	Axial mode number (k_ℓ/π)
M	Mach number
M_o'	Magnitude of Mach number perturbation at head end of chamber
N	Dimensionless expression defined by Eq. 34
$\hat{n}$	Normal unit vector
p	Pressure
Q	Resonance quality factor
R	Radius of chamber

r Dimensionless radius (r/L)

S_c Cross-sectional area of chamber

S_p Nozzle entrance area

s Dimensionless entropy $(\eta - \rho'/\bar{\rho})$

t Time; non-dimensional following Eq. 2 [(real time)/(L/a)]

u Velocity

X Square of the absolute value of complex non-dimensional nozzle admittance $(\mu^2 + \theta^2)$

x Dimensional axial distance from head end of chamber

Z Dimensionless head-end impedance (η/M_o')

z Dimensionless length measured from head end of chamber (x/L)

α Attenuation constant, also dimensionless group in Eq. 43 and real part of ϕ (Eq. 45)

β Dimensionless group in Eq. 43, also imaginary part of ϕ (Eq. 45)

γ Ratio of specific heats

δ Shift from closed tube resonant frequency due to the presence of a nozzle $(\Omega_p - \ell\pi)$

ϵ Shift from resonant frequency at half-power point $\left[\pm(\Omega_p - \Omega_{\frac{1}{2}})\right]$

ζ Non-dimensional space coordinate in a moving coordinate system $(z - M_c t)$

η Non-dimensional pressure $(p'/\gamma\bar{p})$

θ Imaginary part of non-dimensional nozzle admittance

Λ Imaginary part of k

λ Wavelength

μ Real part of non-dimensional nozzle admittance

ρ Density

τ Non-dimensional time (used in variable transformation)

ϕ Phase angle between velocity and pressure perturbations, also $\tan^{-1}h(-A_n)$, see Eq. 29

ψ_ℓ Classical closed chamber pressure mode for purely axial oscillations

ψ_N Classical closed chamber pressure mode

Ω Real part of k

$\bar{\Omega}$ Non-dimensional frequency defined as $\Omega/(1 - M_c)^2$

ω Dimensional angular frequency

SUBSCRIPTS

c Chamber property

ℓ Pure axial mode

max Maximum value

N Classical closed chamber mode

n Nozzle condition

o Head-end condition

p Peak value

r Real part of complex quantity

\+ Wave traveling in positive direction

\- Wave traveling in negative direction

$\frac{1}{2}$ Half-power point

SUPERSCRIPTS

(i) Imaginary part of complex expression

(r) Real part of complex expression

′ Perturbation quantity

\- Mean value

→ Vector quantity

I. INTRODUCTION

An understanding of the behavior of waves in a rocket chamber rests essentially on knowledge of the various sources and sinks of energy. The primary source of energy is of course the propellant itself and the driving mechanism is associated with a coupling between the wave motions and the combustion process. It appears possible to isolate this aspect of the problem, so far as solid propellant rockets are concerned, not only analytically, but also experimentally (Ref. 1 and 2). With sufficient development, the T-burner and L*-burner may provide adequate means for studying the coupling (interpreted often as an "admittance function") without firing a complete rocket.

But the source of energy is only half of the problem. It is always present, and in order that a rocket burn stably, there must exist ways for wave energy to be dissipated at a rate greater than that at which the combustion process provides energy. In some respects, it is theoretically more difficult to assess the losses than the gains. Indeed, it is possible to compute much of the energy losses only for relatively simple geometries, and even in those cases, approximations are necessary. Hence one would like also to be able to measure the losses separately.

Since the losses associated with a chamber are strongly influenced by the geometry, which in turn affects the mean flow, it is in fact necessary to work with a chamber, perhaps scaled down. The problem is simplified by using an external source of cold gas, rather than burning, for the flow in the rocket. Acoustic oscillations may be excited, also by external means, and the attenuation of the waves inferred in a manner described below. Perhaps the simplest example of this kind of device is illustrated in Fig. 1 (see Ref. 3 and 4). The chamber is fitted with a nozzle which normally is choked. Air flows through the porous plate at the head end, and oscillations are excited by a rotary valve upstream of the porous plate. An alternative way is to drive the oscillations with a small speaker.

This configuration evidently simulates an end-burning rocket, which seems quite restrictive. However, the measurements will provide information principally about the damping of waves due to the action of the exhaust end of the chamber, i.e., the effect of the nozzle and also nonuniformities in the flow just upstream of the nozzle entrance. It is not possible to separate these in the experiments. Clearly the results are applicable to other kinds of rockets having similar exhaust configurations. The more serious limitation is that in the measurements reported

in Ref. 3 and 4, only axial modes have been treated. In this report as well, only axial modes will be discussed, but much of the treatment can be extended to radial and tangential modes.

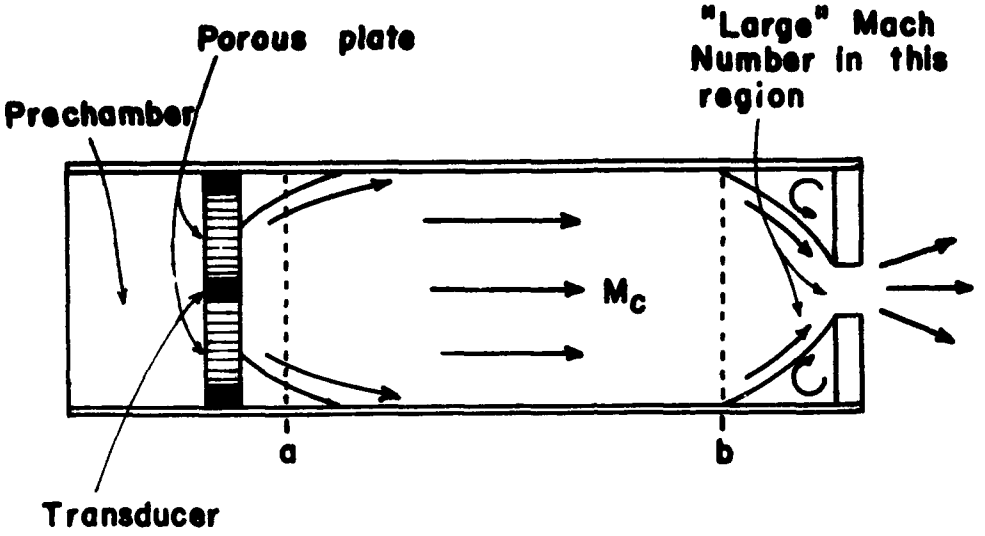

FIG. 1. Sketch of a Cold-Flow Rocket.

The following remarks are concerned with an analysis of the axial modes, with a purely axial mean flow. It is not the intent here to compute the actual damping to be expected, for in fact this can be done only for simple cases. Rather, it is more important to determine how the formal analysis can be used as an aid to interpreting the experimental data, thereby yielding useful numerical results which cannot be obtained by calculation alone.

First, a relatively general treatment of the problem will be covered, based on earlier work (Ref. 5); this leads to formulas for the frequency and attenuation coefficient for freely decaying waves. Then traveling and standing waves in a uniform mean flow will be treated. The analysis is specifically for the case when waves are driven at one end of the chamber. Formulas for the frequency response and the standing wave ratio are found. Perhaps the most important result is the relation between the attenuation coefficient and the properties of the frequency response. The conditions under which the familiar definition of "Q" is valid are found.

The three calculations mentioned in the previous paragraph correspond to the three kinds of measurements most easily made: direct measurement of the attenuation of waves, the frequency response, and amplitude of

of pressure as a function of position in the chamber (i.e., standing wave ratio). Thus the results are immediately applicable to experimental work.

II. GOVERNING EQUATIONS FOR ACOUSTIC OSCILLATIONS IN COLD-FLOW ROCKETS

A rather general analysis of acoustic oscillations in rocket chambers exists (Ref. 5) and it will be specialized in this section to the simpler case of a cold-flow rocket with axial mean flow. Only axial modes are discussed, but it is necessary, for a reason apparent shortly, to retain the equations in three-dimensional form. Extension to other modes may be carried out by following the analysis of Ref. 5. It is convenient for the analysis of the acoustics of rocket chambers to use an equation for the pressure rather than temperature, so that the three equations for inviscid flow of a perfect gas are

$$\frac{\partial \rho}{\partial t} + \nabla \cdot (\rho \vec{u}) = 0$$

$$\frac{\partial \vec{u}}{\partial t} + \vec{u} \cdot \nabla \vec{u} + \frac{\nabla p}{\rho} = 0$$

$$\frac{\partial p}{\partial t} + \gamma p \nabla \cdot \vec{u} + \vec{u} \cdot \nabla p = 0$$

The last may be found by combining the usual energy equation with the continuity equation. In the usual way, all quantities are written as sums of mean values, independent of time but in general functions of position, and fluctuations which vary with both time and position in the chamber. The complete perturbation equations may be put in the form

$$\frac{\partial \vec{u}'}{\partial t} + \bar{\vec{u}} \cdot \nabla \vec{u}' + \vec{u}' \cdot \nabla \bar{\vec{u}} + \nabla(a^2 \eta) + \frac{s'}{c_p} \frac{\nabla \bar{p}}{\bar{\rho}} = 0 \qquad (1)$$

$$\frac{\partial p'}{\partial t} + \gamma p' \nabla \cdot \bar{\vec{u}} + \gamma \bar{p} \nabla \cdot \vec{u}' + \bar{\vec{u}} \cdot \nabla p' + \vec{u}' \cdot \nabla \bar{p} = 0 \qquad (2)$$

where a is the mean speed of sound, $\eta = p'/\gamma\bar{p}$, and $s' = \eta - \rho'/\bar{\rho}$ is the fluctuation of entropy. For applications to the low Mach number flow in a cold rocket, it is not necessary to include variations in the mean pressure and temperature. The equations have the simpler form

$$\frac{\partial \vec{M}'}{\partial t} + \vec{\bar{M}} \cdot \nabla \vec{M}' + \vec{M}' \cdot \nabla \vec{\bar{M}} + \nabla \eta = 0 \tag{3}$$

$$\frac{\partial \eta}{\partial t} + \vec{\bar{M}} \cdot \nabla \eta + \gamma \eta \nabla \cdot \vec{\bar{M}} + \nabla \cdot \vec{M}' = 0 \tag{4}$$

All variables are now dimensionless; t is the real time divided by L/a, L being the length of the chamber, $\vec{\bar{M}} = \vec{\bar{u}}/\bar{a}$, $\vec{M}' = \vec{u}'/\bar{a}$, and all lengths are normalized with respect to L. Hereafter, $\nabla \cdot \vec{\bar{M}} = 0$ will be assumed. This is a consequence of the low speeds involved, but it cannot be assumed if there is combustion in the chamber.

III. APPROXIMATE SOLUTION FOR THE FREQUENCY AND ATTENUATION OF STANDING WAVES

The results obtained in this section will apply to waves which are <u>not</u> driven by external means. A wave equation for η is found in the usual way by taking the time derivative of Eq. 4 and substituting Eq. 3 for $\partial \vec{M}'/\partial t$

$$\nabla^2 \eta - \frac{\partial^2 \eta}{\partial t^2} = \vec{\bar{M}} \cdot \nabla \frac{\partial \eta}{\partial t} - \nabla \cdot \left[\vec{\bar{M}} \cdot \nabla \vec{M}' + \vec{M}' \cdot \nabla \vec{\bar{M}} \right]$$

The boundary conditions on η are set in accord with Eq. 3

$$\nabla \eta = - \frac{\partial \vec{M}'}{\partial t} - \left[\vec{\bar{M}} \cdot \nabla \vec{M}' + \vec{M}' \cdot \nabla \vec{\bar{M}} \right]$$

For ease in writing, the last two equations will be written, in the case of steady waves, as

$$\nabla^2 \eta + k^2 \eta = h \tag{5}$$

$$\hat{n} \cdot \nabla \eta = -f \text{ (on } z = 0, z = 1) \tag{6}$$

where

$$h = ik\vec{\bar{M}} \cdot \nabla \eta - \nabla \cdot \left(\vec{\bar{M}} \cdot \nabla \vec{M}' + \vec{M}' \cdot \nabla \vec{\bar{M}} \right) \tag{7}$$

$$f = ikA\eta + \left(\vec{\bar{M}} \cdot \nabla \vec{M}' + \vec{M}' \cdot \nabla \vec{\bar{M}} \right) \cdot \hat{n} \tag{8}$$

The unknown boundary values of the Mach number (or velocity) fluctuations have been replaced in Eq. 8 by admittance functions A defined so that the normal components of the fluctuations are proportional to the pressure fluctuations,

$$\vec{M}' \cdot \hat{n} = A\eta \tag{9}$$

In general, A is a complex function, $A = A^{(r)} + iA^{(i)} = |A|e^{i\phi}$, so that the real part gives that part of the normal velocity fluctuation u_r which is in phase with the pressure: $u_r' = \left(A^{(r)}\frac{\bar{a}}{\gamma\bar{p}}\right)p'$. But the rate at which work is done on or by the waves at the end surfaces is $u_r'p' = A^{(r)}\frac{\bar{a}}{\gamma\bar{p}}(p')^2$. Consequently, it is the real part of the admittance function which will be related to the damping of the waves.

For the cases treated here (and usually in rocket chambers), the boundaries and the mean flow cause only small perturbations from the classical closed chamber modes Ψ_N which satisfy the equations

$$\nabla^2\Psi_N + k_N^2\Psi_N = 0 \tag{10}$$

$$\hat{n} \cdot \nabla\Psi_N = 0 \quad \begin{cases} z = 0, 1 \\ r = R/L \end{cases} \tag{11}$$

where R is the radius of the cylindrical chamber. For these modes in a closed chamber, the normal gradient of pressure vanishes at the ends, since $\nabla p' = \gamma\bar{p}\nabla\eta = \gamma\bar{p}\nabla\Psi_N$ here. But by Eq. 3 with $\bar{M} = 0$ and $\vec{M}'$ varying harmonically

$$(\partial\vec{M}'/\partial t = ik\vec{M}'),\ \vec{M}' = -\nabla\eta/ik, \text{ or } \vec{u}' = -\frac{\bar{a}}{ik}\nabla\eta = -\frac{\bar{a}}{ik}\nabla\Psi_N$$

Hence since $\hat{n} \cdot \nabla\Psi_N$ vanishes on the boundary, so does the normal component of the velocity fluctuation. In the case of purely axial oscillations, $\Psi_N = \cos(k_\ell z)$ with $k_\ell = \ell\pi$, $\ell = 1, 2, \cdots$. The idea of the following computation is that even with a nozzle or a porous head end, the mode shapes are not much changed from these classical vibrations; this is true if the mean flow Mach number is small and if the admittance functions are small. It is not generally true if the oscillations are driven at the head end, for the velocity fluctuation at that end may be given any value and, correspondingly, the frequency may be changed at will.

The computation here is directed to determining the corrections to $k_\ell = \ell\pi$ due to the mean flow and damping within the chamber or at the boundaries. It is a simple matter to compute the first-order approximation

to k (the mean-flow Mach number is the small parameter). Multiply Eq. 5 by Ψ_N, Eq. 10 by η and subtract the equations; then integrate over the volume of the chamber:

$$\iiint \left(\Psi_N \nabla^2 \eta - \eta \nabla^2 \Psi_N\right) dv + \left(k^2 - k_N^2\right) \iiint \Psi_N \eta dv = \iiint \Psi_N \, h dv$$

The volume integral on the left-hand side may be transformed by use of Green's theorem, and Eq. 6 and 11 used for the surface conditions. One finds

$$k^2 = k_N^2 + \frac{1}{\iiint \Psi_N \eta dv} \left(\iiint \Psi_N h dv + \iint f \Psi_N ds \right) \tag{12}$$

There are really two surface integrals involving f--one over the plane z = 0 and one over z = 1.

To obtain a first-order approximation for the right-hand side, the zeroth order approximation for η, $\eta \approx \Psi_N$ is used. In the case of purely axial oscillations, $\Psi_N = \cos(k_\ell z)$ with $k_\ell = \ell\pi$, and if one assumes $\vec{M}$ to be axial only, $\vec{M} = \bar{M}\hat{e}_z$, then h and f are approximately (i.e., to order $\bar{M}$)

$$h = ik\bar{M} \frac{d\Psi_\ell}{dz} - \frac{i}{k_\ell} \frac{d^2}{dz^2} \left(\bar{M} \frac{d\Psi_\ell}{dz} \right) \tag{13}$$

$$f = ikA\Psi_\ell + \frac{i}{k_\ell} \frac{d}{dz} \left(\bar{M} \frac{d\Psi_\ell}{dz} \right) \tag{14}$$

where the zeroth order approximation, derived from Eq. 3, has been used used for $\vec{M}'$: $M' \approx (i/k_\ell)(d\Psi_\ell/dz)$. (Note that the exponential time factor $\exp(i\omega t) = \exp[i(\omega L/a) \cdot (at/L)]$ is $\exp(ikt)$ in dimensionless form, and to zeroth order $k = k_\ell = \ell\pi$.) The volume integral in Eq. 12 may now be simplified by carrying out the integral over z with some use of the fact that $d^2\Psi_\ell/dz^2 = -k_\ell^2 \Psi_\ell$. One finds

$$\iiint \Psi_\ell h dv \approx ik_\ell \left(\iint \bar{M} \Psi_\ell^2 ds \right)_0^1$$

The surface integral, over z = 0 and z = 1, gives

$$\iint \Psi_\ell f ds = \left(\iint \Psi_\ell f ds\right)_{z=1} + \left(\iint \Psi_\ell f ds\right)_{z=0}$$

$$= ik_\ell \left[\left(\iint A\Psi_\ell^2 ds\right)_{z=1} + \left(\iint A\Psi_\ell^2 ds\right)_{z=0}\right] - ik_\ell \left[\iint \bar{M}\Psi_\ell^2 ds\right]_0^1$$

After these results have been used in Eq. 12 the real and imaginary parts of $k = \Omega + i\Lambda$ are, to first order in $\bar{M}$,*

$$\Omega^2 = k_\ell^2 - 2k_\ell \left(\iint A_o^{(i)} \Psi_\ell^2 \frac{ds}{S_c} + \iint A_n^{(i)} \Psi_\ell^2 \frac{ds}{S_c}\right) \tag{15}$$

$$\Lambda = \iint A_o^{(r)} \Psi_\ell^2 \frac{ds}{S_c} + \iint A_n^{(r)} \Psi_\ell^2 \frac{ds}{S_c} \tag{16}$$

in which S_c is the cross-sectional area of the chamber and $A = A^{(r)} + iA^{(i)}$ in complex form. The admittance function for the nozzle end is A_n and at the head end it is A_o.

It is now apparent why the calculations were not immediately reduced to one-dimensional form. If that step had been taken, then the important (and obvious) result that the surface integrals must be weighted by the appropriate areas would not have appeared. Thus, for example, if the nozzle entrance area is S_p, the damping term in Eq. 16 is $A_n^{(r)} S_p/S_c$, since $\Psi_\ell^2 = 1$ at $z = 1$.

The formulas 15 and 16 are valid for the axial modes with one-dimensional mean flow, subject to the restriction that the Mach number of the mean flow must be small. Hence, care must be taken when these are used for a rocket with an abrupt change of cross section, from the port area to a sonic nozzle as sketched in Fig. 1. There are evidently regions of rapid variations in mean-flow properties near the porous head plate and near the nozzle. Average streamlines have been sketched. The expressions 15 and 16 are valid only in the region between the planes at a and b, between which the Mach number is approximately constant, equal to M_c when there is no burning.

It appears that the region near the porous plate may be so thin that as an approximation, position a is in fact at the origin, and the

---

* Note that $\int_0^1 \Psi_\ell^2 dz = \frac{1}{2}$ for $\ell \neq 0$.

admittance function is then non-zero over the porous area (S_p) at most (the velocity fluctuation is elsewhere zero on z = 0). But yet the influence of the mean flow may be represented by the average chamber Mach number acting over the entire chamber area. Note that the volume integral of h and the part of f depending on Mach number cancel, which happens only if $\bar{M}$ is constant. This is merely a statement of the fact that if the flow is uniform, the rate of convection of wave energy into the region bounded by two planes normal to the flow is obviously equal to the rate of convection out. Then, if the admittance functions are constant over the corresponding areas, Eq. 15 and 16 become

$$\Omega^2 = k_\ell^2\left[1 - \frac{2}{k_\ell}\left(A_o^{(i)}\frac{S_p}{S_c} + A_n^{(i)}\right)\right] \tag{17}$$

$$\Lambda = A_o^{(r)}\frac{S_p}{S_c} + A_n^{(r)} \tag{18}$$

To first order, then

$$k \approx k_\ell\left[1 + i\left(\frac{S_p}{S_c}A_o + A_n\right)\right]$$

The effects at the exhaust end, including rapid acceleration to the sonic throat and eddies of some sort which must exist in the corners of the chamber, have been included in A_n. It is obviously not reasonable to calculate this quantity which is more than just the nozzle admittance function. But, on the other hand, if one tries to extend the region in which the standing waves exist (i.e., b → 1), then the equations for the waves must be seriously complicated, both because $|\bar{M}|$ is not small and because $\vec{M}$ is no longer in the axial direction. The analysis by Cantrell, McClure, and Hart (Ref. 6) is of course subject to the same restrictions. If the nozzle convergent fairs more or less smoothly to the chamber, then A_n is indeed almost entirely the nozzle admittance function, which can be calculated independently.

It is these difficulties which lead one to use the analysis as a guide to interpretation of experimental results, rather than as a means of thorough computation. According to Eq. 16 and 17, the amplitude of a wave varies with time as

$$p' = e^{ikt} = \exp\left[-\left(A_o^{(r)}\frac{S_p}{S_c} + A_n^{(r)}\right)t\right]\exp\left\{ik_\ell\left[1 - \frac{2}{k_\ell}\left(A_o^{(i)}\frac{S_p}{S_c} + A_n^{(i)}\right)\right]^{\frac{1}{2}}t\right\}$$

In terms of dimensional quantities, the attenuation constant α is therefore

$$\alpha = \frac{a}{L}\left(A_n^{(r)} + A_o^{(r)}\frac{S_p}{S_c}\right)\text{sec}^{-1} \tag{19}$$

and the angular frequency of freely decaying waves is

$$\omega = \ell\pi\frac{a}{L}\left[1 - \frac{2}{\ell\pi}\left(A_n^{(i)} + A_o^{(i)}\frac{S_p}{S_c}\right)^2\right]^{\frac{1}{2}}\text{sec}^{-1} \tag{20}$$

$$= \ell\pi\frac{a}{L}\left[1 - \frac{1}{\ell\pi}\left(A_n^{(i)} + A_o^{(i)}\frac{S_p}{S_c}\right)\right]\text{sec}^{-1}$$

Equations 19 and 20 are applicable to, for example, experiments involving the explosion of a small charge and measurement of the decay rate and frequency of subsequent waves. They are valid, in fact, for a port of any shape so long as it is straight. If the Mach number is not uniform, some of the integrals in Eq. 15 and 16 contribute additional terms.

IV. WAVES WITH UNIFORM MEAN FLOW

For studying the frequency response when waves are driven, it is best to incorporate at the very beginning the fact that the mean flow is uniform (although as in the previous section, the cross section of the chamber need not be circular). The governing first-order equations for M', the axial Mach number fluctuation, and η, are

$$\frac{\partial M'}{\partial t} + M_c\frac{\partial M'}{\partial z} + \frac{\partial \eta}{\partial z} = 0 \tag{21}$$

$$\frac{\partial \eta}{\partial t} + M_c\frac{\partial \eta}{\partial z} + \frac{\partial M'}{\partial z} = 0 \tag{22}$$

in which M_c is the Mach number of flow in the chamber. The case of transient decay of waves, i.e., the transient response of the chamber, has already been treated, with the results given in Eq. 19 and 20. In this section, the analysis of the frequency response is begun.

By analogy with the familiar ideas of "lumped" electrical circuits and mechanical systems, one expects the width of the peak in the frequency response to be proportional to the attenuation constant, Eq. 19, associated with the transient response. Some experiments (Ref. 3 for example) have in fact shown quite good agreement, but it is not obvious why this should be so. Indeed, the calculations here indicate that the

agreement may imply that the admittance function for the porous plate (and hence the associated attenuation) is negligible compared to the effects of the exhaust end of the chamber. This was intended to be the case in the experiments (Ref. 4).

When standing waves are sustained by external means, the analysis is often instructively cast in terms of traveling waves (as, for example, in the problem of a transmission line which the present problem closely resembles). If one performs the coordinate transformation

$$\tau = t$$

$$\zeta = z - M_c t$$

then Eq. 21 and 22 become

$$\frac{\partial M'}{\partial \tau} + \frac{\partial \eta}{\partial \zeta} = 0$$

$$\frac{\partial \eta}{\partial \tau} + \frac{\partial M'}{\partial \zeta} = 0$$

which imply the wave equations

$$\left(\frac{\partial^2}{\partial \zeta^2} - \frac{\partial^2}{\partial \tau^2}\right)\begin{pmatrix} M' \\ \eta \end{pmatrix} = 0 \tag{23}$$

Obviously then, one has two solutions, corresponding to waves traveling to the left and to the right. Alternatively, the wave equations in t, z coordinates are

$$\left[\left(1 - M_c^2\right)\frac{\partial^2}{\partial z^2} - 2M_c \frac{\partial^2}{\partial z \partial t} - \frac{\partial^2}{\partial t^2}\right]\begin{pmatrix} M' \\ \eta \end{pmatrix} = 0 \tag{24}$$

In any case, the complete solutions can be written

$$\eta = e^{i\Omega t}\left[\eta_+ e^{-i\frac{\Omega}{1 + M_c} z} + \eta_- e^{i\frac{\Omega}{1 - M_c} z}\right] \tag{25}$$

$$M' = e^{i\Omega t}\left[M_+ e^{-i\frac{\Omega}{1 + M_c} z} + M_- e^{i\frac{\Omega}{1 - M_c} z}\right] \tag{26}$$

Note that the frequencies of the two waves are not the same: $\Omega_+ = \Omega/(1 + M_c)$ for the wave to the right, and $\Omega_- = \Omega/(1 - M_c)$ for the

wave to the left. This is the "Doppler effect" often mentioned in the literature of acoustics applied to rockets, but not usually shown. A wave of frequency Ω in the laboratory and traveling in the direction of the moving stream has a lower frequency with respect to the stream. Substitution of these expressions into one of the first-order Eq. 21 or 22 shows that

$$M_+ = \eta_+$$

$$M_- = -\eta_- \tag{27}$$

Now in the case of the cold-flow rocket experiments, the waves are driven at the head end. A solution corresponding to the standing wave existing at any frequency is obtained by superposing the correct amount of + and - waves to satisfy the boundary condition at the exhaust end, assumed here to be at a plane as suggested by Fig. 1 and associated remarks. One can imagine that a wave traveling to the right is partly reflected and partly transmitted; the amplitude and phase of the reflected wave is so determined as to have a standing wave observed in the laboratory. The ratio of amplitudes of the impinging and reflected waves is usually called the "standing wave ratio." In accord with previous remarks, let all effects at the exhaust end be represented by the admittance function A_n, so that at $z = 1$

$$M'/\eta = A_n \tag{28}$$

The plane $z = 1$ is actually slightly displaced from the end plate--it is labeled b in Fig. 1. Note again that A_n includes more than simply the nozzle admittance function. Hence Eq. 25-27 imply

$$\frac{\eta_+ e^{-i\bar{\Omega}} - \eta_- e^{i\bar{\Omega}}}{\eta_+ e^{-i\bar{\Omega}} + \eta_- e^{i\bar{\Omega}}} = A_n$$

where $\bar{\Omega} = \Omega/(1 - M_c^2)$ and use has been made of the fact that

$$\frac{\Omega}{1 - M_c} = M_c\bar{\Omega} + \bar{\Omega}, \quad \frac{\Omega}{1 + M_c} = -M_c\bar{\Omega} + \bar{\Omega}$$

Hence the complex amplitude of the wave traveling to the left is

$$\eta_- = \eta_+ \frac{1 - A_n}{1 + A_n} e^{-2i\bar{\Omega}}$$

and the solutions for η, M' are

$$\eta = \eta_+ e^{i\Omega t \pm i\bar{\Omega}M_c z - i\bar{\Omega}}\left[e^{-i\bar{\Omega}(z-1)} + \frac{1 - A_n}{1 + A_n} e^{i\bar{\Omega}(z-1)}\right]$$

$$M' = \eta_+ e^{i\Omega t + i\bar{\Omega}M_c z - i\bar{\Omega}}\left[e^{-i\Omega(z-1)} - \frac{1 - A_n}{1 + A_n} e^{i\bar{\Omega}(z-1)}\right]$$

which can also be written as

$$\eta = \frac{2\eta_+}{A_n + 1} e^{i\Omega t + i\bar{\Omega}(M_c z - 1)}\left[\cos\bar{\Omega}(z-1) - iA_n \sin\bar{\Omega}(z-1)\right]$$

$$M' = \frac{2\eta_+}{A_n + 1} e^{i\Omega t + i\bar{\Omega}(M_c z - 1)}\left[A_n \cos\bar{\Omega}(z-1) - i\sin\bar{\Omega}(z-1)\right]$$

Now define ϕ by $\tanh\phi = -A_n$ and

$$\eta = \frac{2\eta_+}{(A_n + 1)\cosh\phi} e^{i\Omega t + i\bar{\Omega}(M_c z - 1)} \cosh\left[i\bar{\Omega}(z-1) + \phi\right] \qquad (29)$$

$$M' = -\frac{2\eta_+}{(A_n + 1)\cosh\phi} e^{i\Omega t + i\bar{\Omega}(M_c z - 1)} \sinh\left[i\bar{\Omega}(z-1) + \phi\right] \qquad (30)$$

These results will be used to describe interpretation of measurements of the steady-state frequency response and of the amplitude of oscillations along the chamber axis.

V. FREQUENCY RESPONSE

The measurements have been made of pressure at the head end. It may be supposed that the oscillations are driven by fluctuations in velocity, or Mach number, at the head end. Thus, let $M' = M_o' e^{i\Omega t}$ at $z = 0$, and Eq. 29 gives

$$\frac{2\eta_+}{\cosh\phi(A_n + 1)} = \frac{-M_o' e^{i\bar{\Omega}}}{\sinh(\phi - i\bar{\Omega})}$$

Then the measured frequency response is represented by

$$\frac{\eta}{M_o'} = -e^{i\bar{\Omega}M_c z} \frac{\cosh\left[i\Omega(z-1)+\phi\right]}{\sinh\left(\phi - i\bar{\Omega}\right)} \tag{31}$$

In particular, at z = 0,

$$\left(\frac{\eta}{M_o'}\right)_{z=0} = -\frac{\cosh\left(\phi - i\bar{\Omega}\right)}{\sinh\left(\phi - i\bar{\Omega}\right)}$$

which can be expanded to

$$\left(\frac{\eta}{M_o'}\right)_{z=0} = \frac{1 + iA_n \tan\Omega}{A_n + i\tan\Omega} \tag{32}$$

It is particularly important to note that since the waves are driven by perturbations at the porous plate, the influence of that region (contained in A_o defined earlier) cannot appear: they are combined with the external driving mechanism to provide, for a given frequency and magnitude of pressure fluctuation, just the value of M_o' required to maintain a steady oscillation. Hence measurements made with a transducer in the porous plate can yield no information about the admittance function to be associated with the porous plate when waves are decaying freely within the chamber. Let $A_n = \mu + i\theta$:

$$\left(\frac{\eta}{M_o'}\right)_{z=0} = \frac{(1 - \theta\tan\Omega) + i(\mu\tan\Omega)}{\mu + i(\theta + \tan\Omega)}$$

and

$$|Z| = \left|\frac{\eta}{M_o'}\right|_{z=0} = \left[\frac{(1-\theta\tan\Omega)^2 + (\mu\tan\Omega)^2}{\mu^2 + (\theta+\tan\Omega)^2}\right]^{\frac{1}{2}} = \sqrt{\frac{N}{D}} \tag{33}$$

where

$$N = X\tan^2\Omega - 2\theta\tan\Omega + 1 \tag{34}$$

$$D = \tan^2\Omega + 2\theta\tan\Omega + X \tag{35}$$

$$X = \mu^2 + \theta^2 \tag{36}$$

The function $|Z(\Omega)|/|Z(\Omega)|_{\Omega=0}$ is plotted in Fig. 2-6 for several representative values of μ and θ. Peaks occur at frequencies $\Omega = \Omega_p$ which, when both μ and θ are small, are close to the frequencies of the natural model for a closed chamber ($\Omega_p \approx \ell\pi$) and close to the frequencies of transient oscillations (Eq. 20) but not necessarily equal to either. The peaks are determined from the condition

$$\frac{d|Z(\Omega)|}{d\Omega} = 0 \tag{37}$$

To simplify calculations, and also to avoid introducing further unknown quantities, suppose that both θ and μ are slowly varying functions of Ω near the peak, then both $d\theta/d\Omega$ and $d\mu/d\Omega$ will be set equal to zero. One finds then that Ω_p is the solution to

$$\tan^2 \Omega_p + \left(\frac{X - 1}{\theta}\right) \tan \Omega_p - 1 = 0 \tag{38}$$

Thus

$$\tan \Omega_p = \frac{1 - X}{2\theta} - \frac{1}{2}\sqrt{\left(\frac{1 - X}{\theta}\right)^2 + 4} \tag{39}$$

The sign on the radical cannot be fixed uniquely. In the limit of small θ and μ the negative sign is the correct choice, for then Eq. 39 gives

$$\tan \Omega_p \approx -\frac{\theta}{1 - X} \approx -\theta$$

and hence

$$\Omega_p \approx \ell\pi - \theta \tag{40}$$

which is exactly the correction, due to the nozzle, shown in Eq. 20 for the frequency of the transient response. On the other hand, peaks do exist for Ω_p far removed from $\ell\pi$; a particularly interesting limit is found by taking the positive sign in Eq. 39, with θ small, for which Eq. 39 becomes

$$\tan \Omega_p \approx \frac{1 - X}{\theta} \approx \frac{1 - \mu^2}{\theta} \tag{41}$$

Let $1 - \mu^2$ be non-zero, and for $\theta \to 0$ the peak frequencies fall in the neighborhood of multiples of $\pi/2$, as shown later by the numerical results.

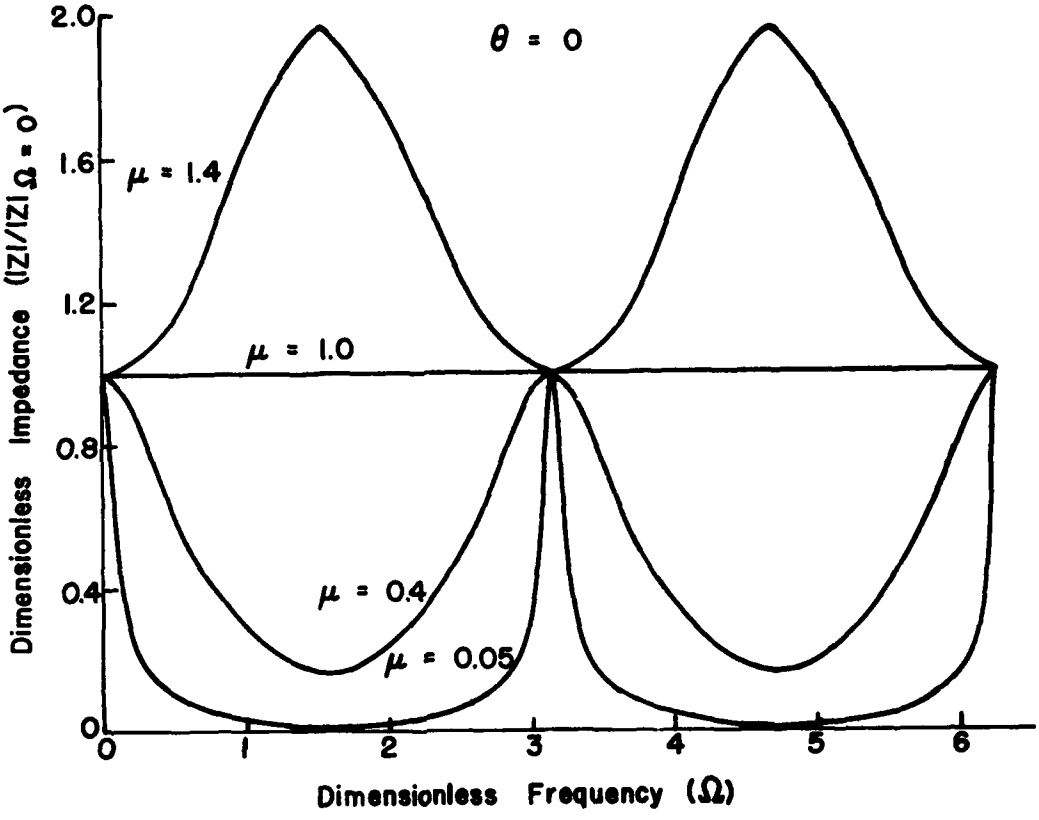

FIG. 2. Dimensionless Impedance at Head End as a Function of Frequency θ = 0.

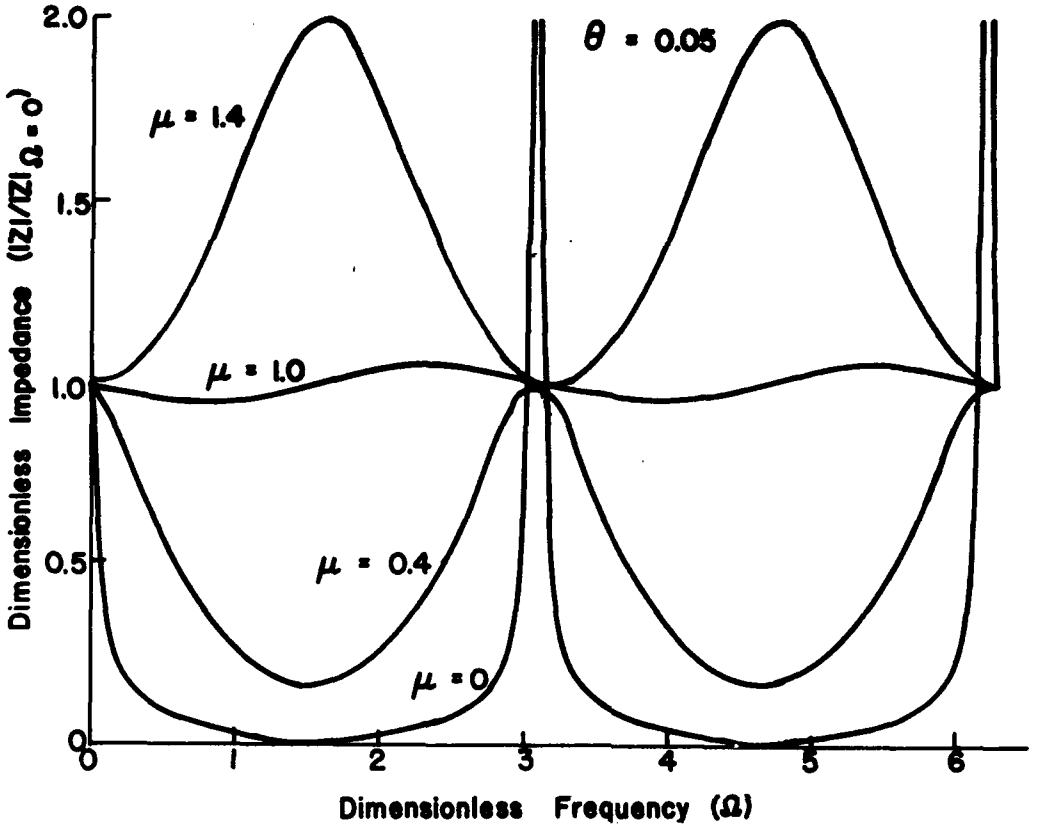

FIG. 3. Dimensionless Impedance at Head End as a Function of Frequency θ = 0.05.

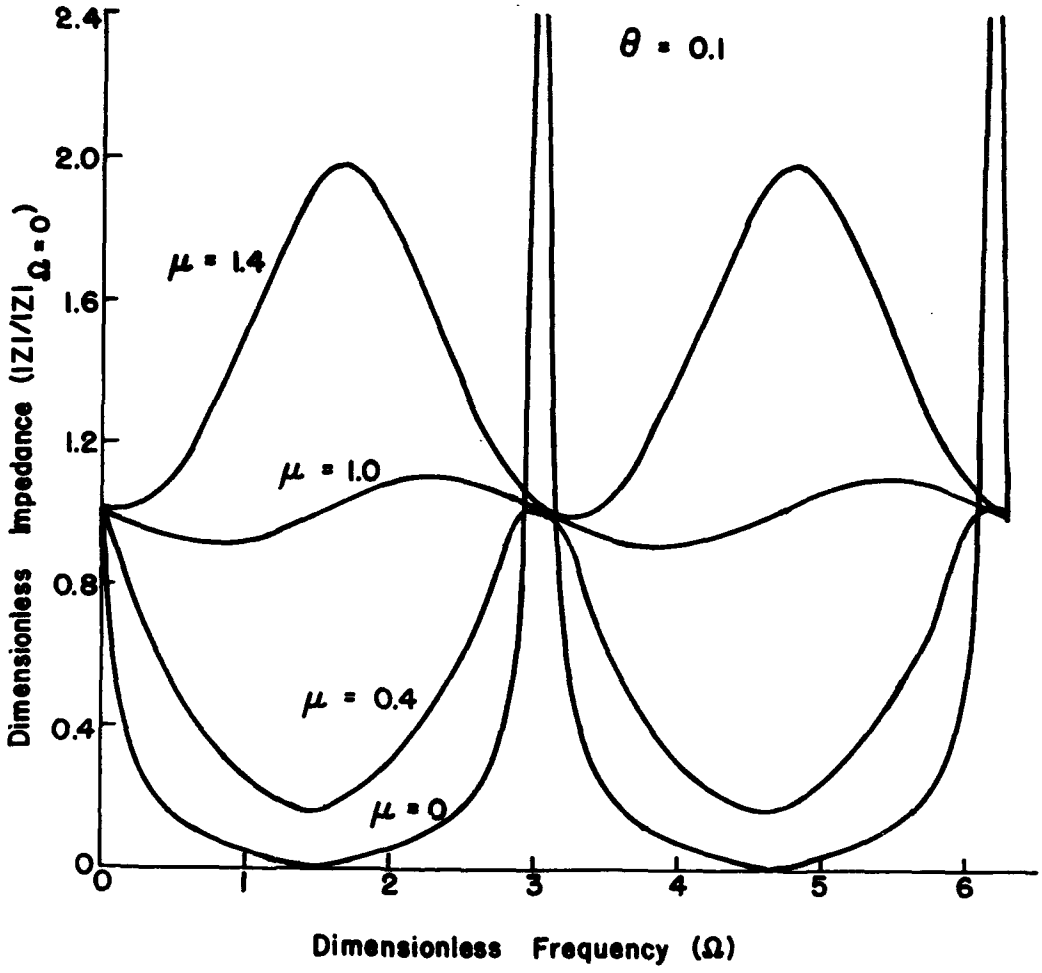

FIG. 4. Dimensionless Impedance at Head End as a Function of Frequency $\theta = 0.1$.

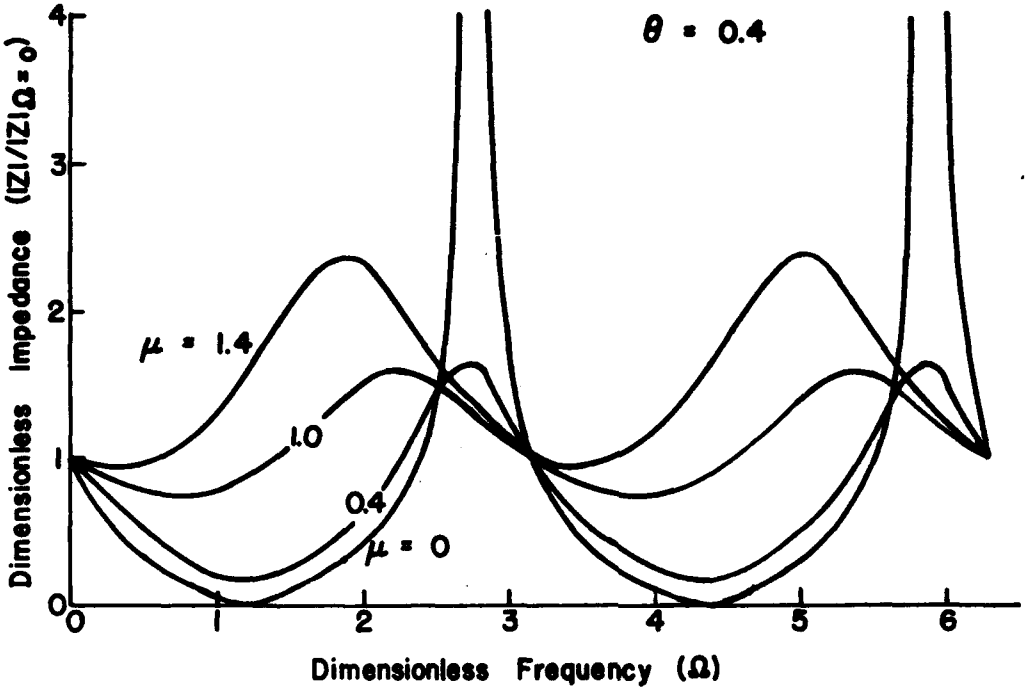

FIG. 5. Dimensionless Impedance at Head End as a Function of Frequency θ = 0.4.

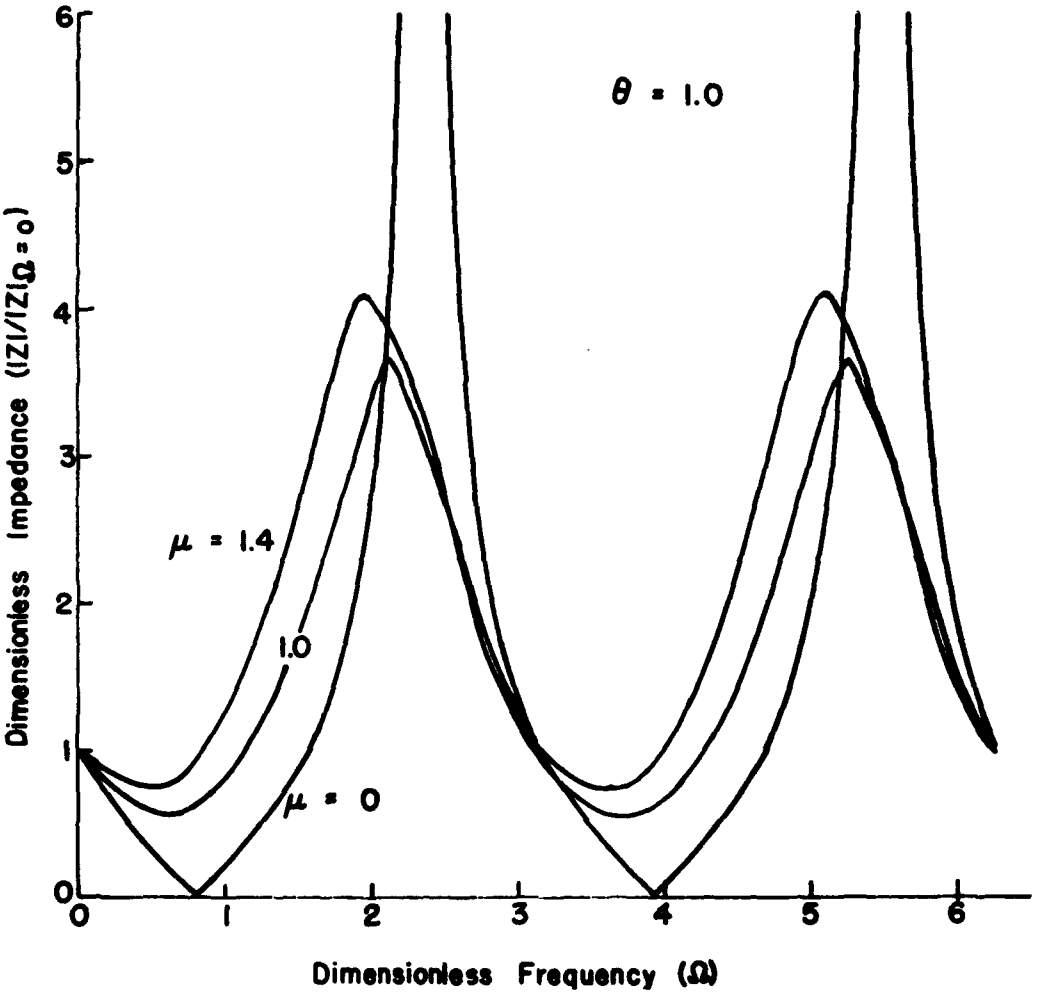

FIG. 6. Dimensionless Impedance at Head End as a Function of Frequency $\theta = 1.0$.

Of greater practical interest is the width of the peak, for one expects by analogy with electrical circuits and simple mechanical systems, that this should be related to the damping of the system. Experiments (Ref. 3 and 4) have shown that the peak is often narrow; the width at the "half-power points," i.e., the frequencies at which $|\bar{\eta}/M_o'|$ is down by $1/\sqrt{2}$ will be denoted by 2ϵ. For θ and μ small, the frequencies at the half-power points are therefore approximately $\ell\pi + \delta \pm \epsilon$. For this limiting case, the peak value of $|Z|$ is

$$|Z|_{max} \approx \left[\frac{(1 + \theta^2)^2 + (\mu\theta)^2}{\mu^2}\right]^{\frac{1}{2}}$$

and the value at the half-power points is

$$|Z|_{\frac{1}{\sqrt{2}}} \approx \left[\frac{[1 - \theta(\epsilon - \theta)]^2 + \mu^2(\epsilon - \theta)^2}{\mu^2 + (\theta + \epsilon - \theta)^2}\right]^{\frac{1}{2}}$$

The condition for finding ϵ is therefore

$$\frac{[1 - \theta(\epsilon - \theta)]^2 + \mu^2(\epsilon - \theta)^2}{\mu^2 + \epsilon^2} \approx \frac{1}{2}\,\frac{(1 + \theta^2)^2 + \mu^2\theta^2}{\mu^2}$$

and one finds

$$\epsilon \approx \pm\,\mu \qquad (\mu, \theta \ll 1)$$

Hence, under these conditions, the width of the peak ($2\epsilon \approx 2\mu$) is twice the attenuation constant for the transient oscillations (Eq. 19) providing the porous plate does not cause much damping of the transient motions (i.e., $A_o^{(r)} = 0$). It follows that in this case, the damping at the exhaust end may indeed be found from $Q = \Omega_p/2\epsilon$; this is valid, then, when the response has a narrow peak, associated with relatively light damping. The attenuation constant is

$$\alpha = \frac{\omega_p}{2Q} = \frac{a}{L}\,\frac{\Omega_p}{2Q} = \frac{a}{L}\,(2\epsilon) \qquad (42)$$

It appears therefore that if agreement is found between the value given by Eq. 41 (i.e., by measurement of the frequency response) and the value given by Eq. 18 (i.e., by measurement of the transient response) then the real part of A_o must be negligibly small. That is, assuming always a lightly damped system, so that the approximations leading to Eq. 40 and 41 are valid, one would conclude that the porous plate contributes insignificant damping.

Not all experiments yield narrow peaks in the frequency response and in those cases the approximate calculation used above is not valid. One cannot compute the transient attenuation constant from the simple formula 42 involving Q. It is necessary to use some sort of graphical procedure such as the following. The values of $|Z|$ at the half-power points are still given by

$$\sqrt{\frac{N}{D}} = |Z|_{\frac{1}{2}} = \frac{1}{\sqrt{2}} |Z|_{max} = \frac{1}{\sqrt{2}} \sqrt{\frac{N_p}{D_p}}$$

where N_p, D_p are the values of N, D for $\Omega = \Omega_p$. This equation, with N and D given by Eq. 34 and 35, leads to a quadratic equation for tan Ω, the tangent of the normalized frequency at the half-power points:

$$\tan^2 \Omega + \tan \Omega \left[\frac{-2\theta(D_p + N_p/2)}{2XD_p - N_p}\right] + \left[\frac{D_p - XN_p/2}{XD_p - N_p/2}\right] = 0 \qquad (43)$$

From Eq. 43 one can find tan Ω and hence Ω at the upper and lower half-power points as functions of μ and θ. The results are conveniently displayed in the forms shown in Fig. 7-10.

Those graphs can be used to determine both the real and imaginary parts of the admittance function at the exhaust end by measurement of the frequency of the peak and the width of the response function. The same information has been cross-plotted in several ways; it is not clear at this time just which form may be most convenient for use in the interpretation of data.

Note that in Fig. 2-6, the impedance has been normalized with respect to its value at zero frequency. Those charts also show a feature remarked upon earlier in connection with Eq. 39, that the frequencies of the peaks need not be close to the values for a closed chamber in the absence of flow. However, it appears that in practice, both μ and θ are small so that in fact Ω_p lies near $\ell\pi$, as shown by Eq. 40.

In Fig. 7, there are several limiting values which should be mentioned. The case $\theta = 0$ yields a resonant frequency of $\ell\pi$ if $\mu < 1$ and $\ell\pi/2$ if $\mu > 1$. This behavior may also be seen in Fig. 2, and follows from Eq. 40 and 41, which show that the switch between values occurs at $\mu = 1$. The limiting case $\theta \to \infty$ can also be extracted from Eq. 41.

A quantity called "maximum half-power bandwidth," equal to π appears in Fig. 8-10. This is also a limiting case, which arises because the impedance Z is precisely periodic in Ω with period π. That the period is π can be shown easily by substituting $\Omega + \pi$ for Ω in Eq. 33. This is exactly true only if μ and θ are both taken to be independent of frequency,

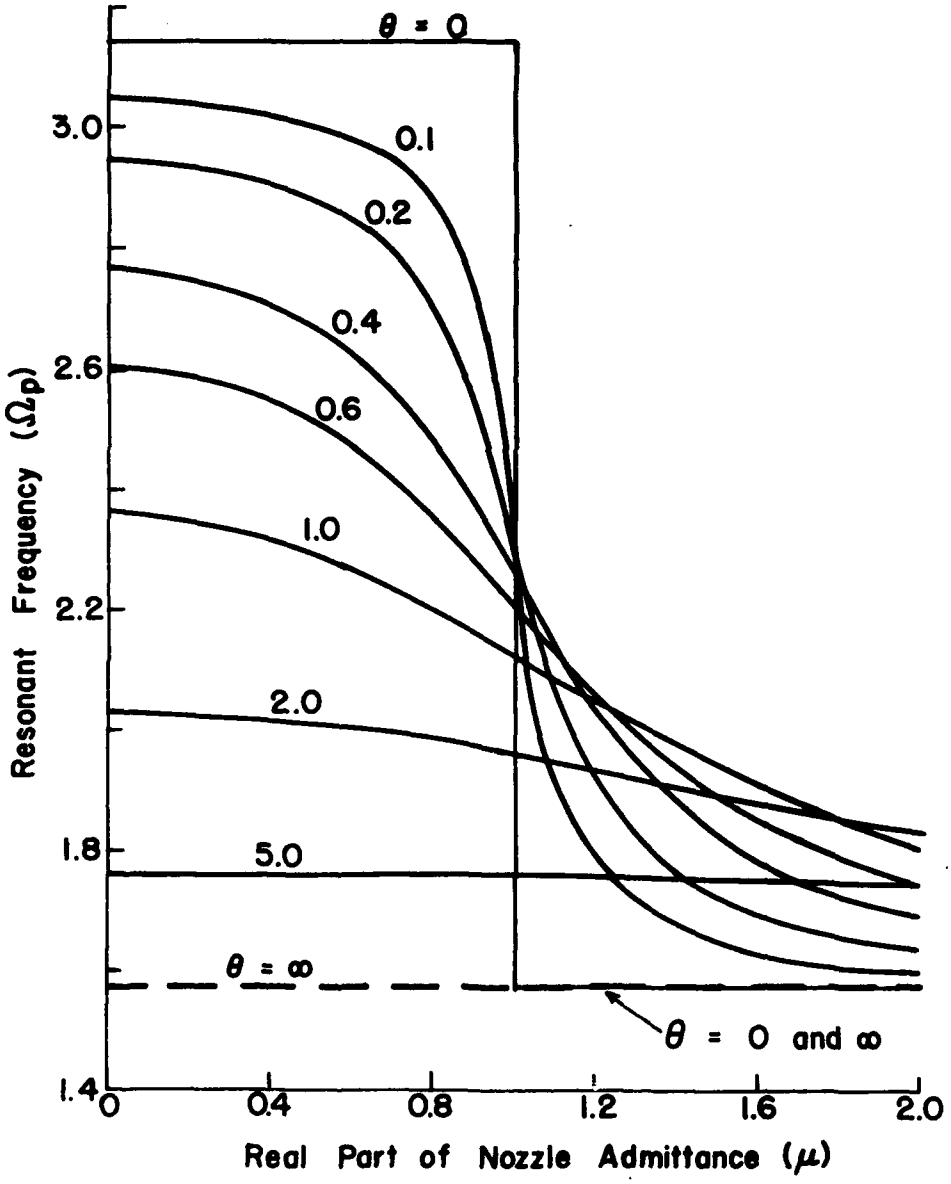

FIG. 7. Frequency at the Maximum Value of the Impedance at the Head End.

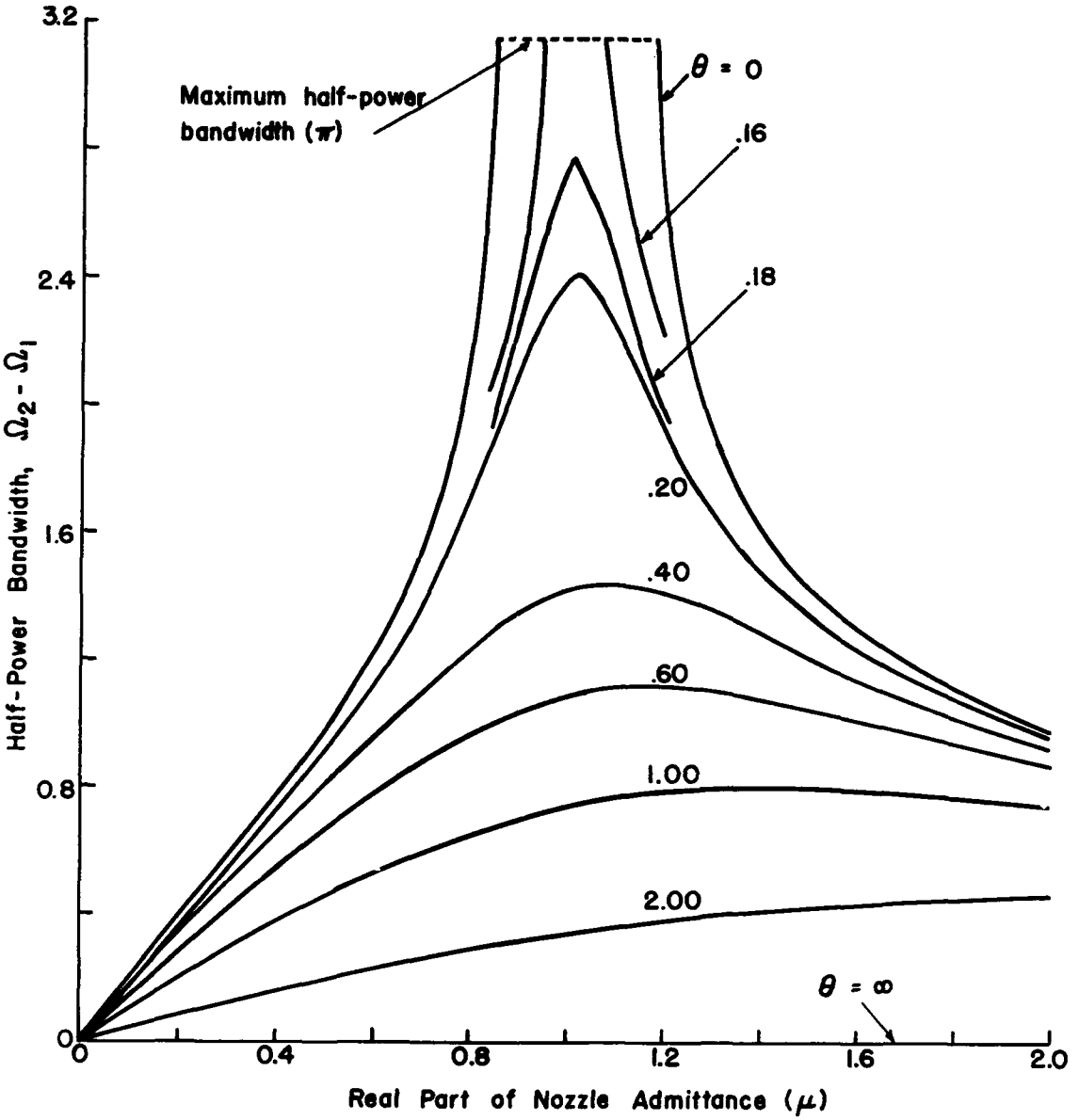

FIG. 8. Half-Power Bandwidth of the Impedance at the Head End.

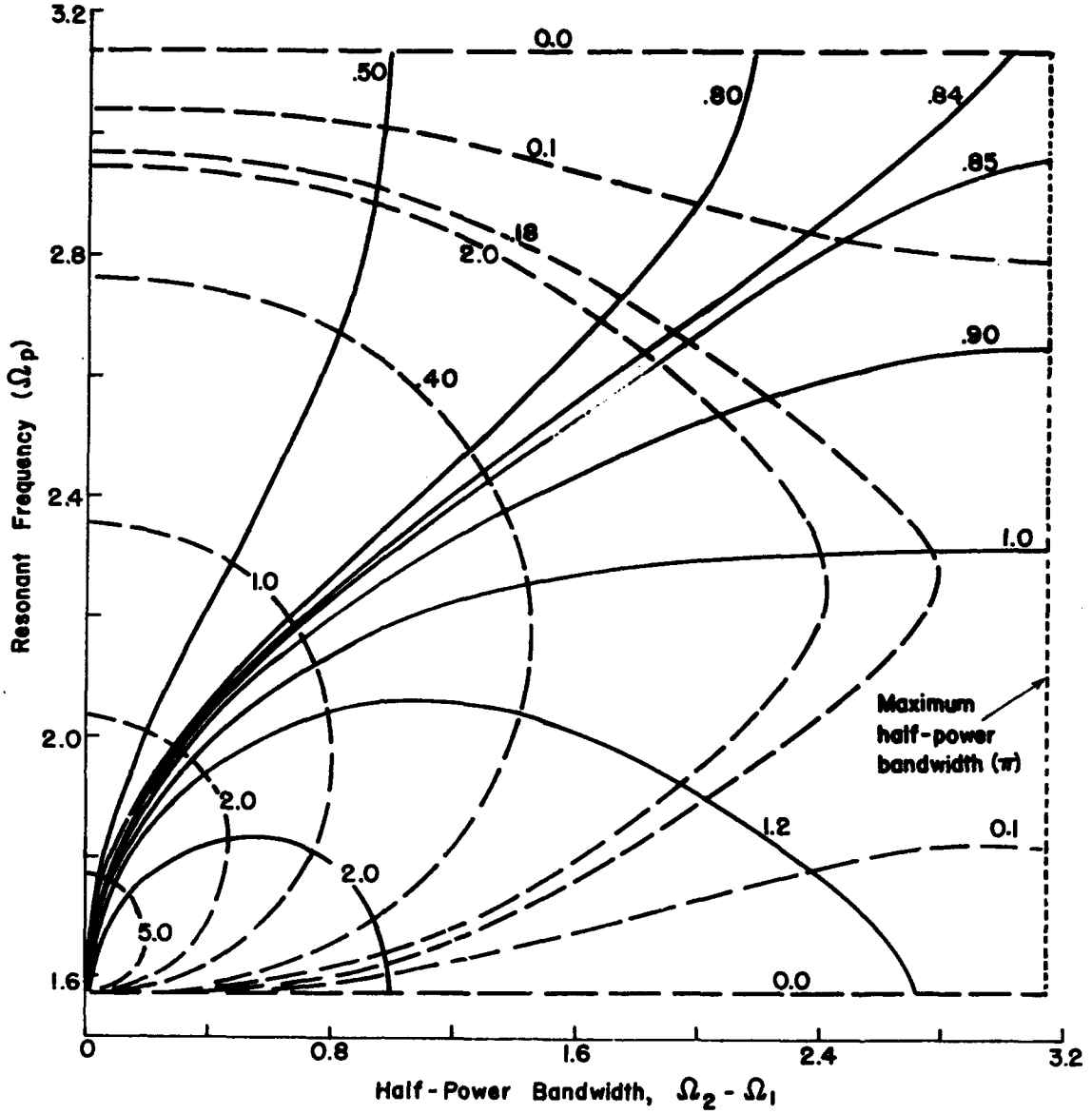

FIG. 9. Frequency at the Maximum Value of the Impedance at the Head End as a Function of Half-Power Bandwidth. (— Constant μ, --- Constant θ.)

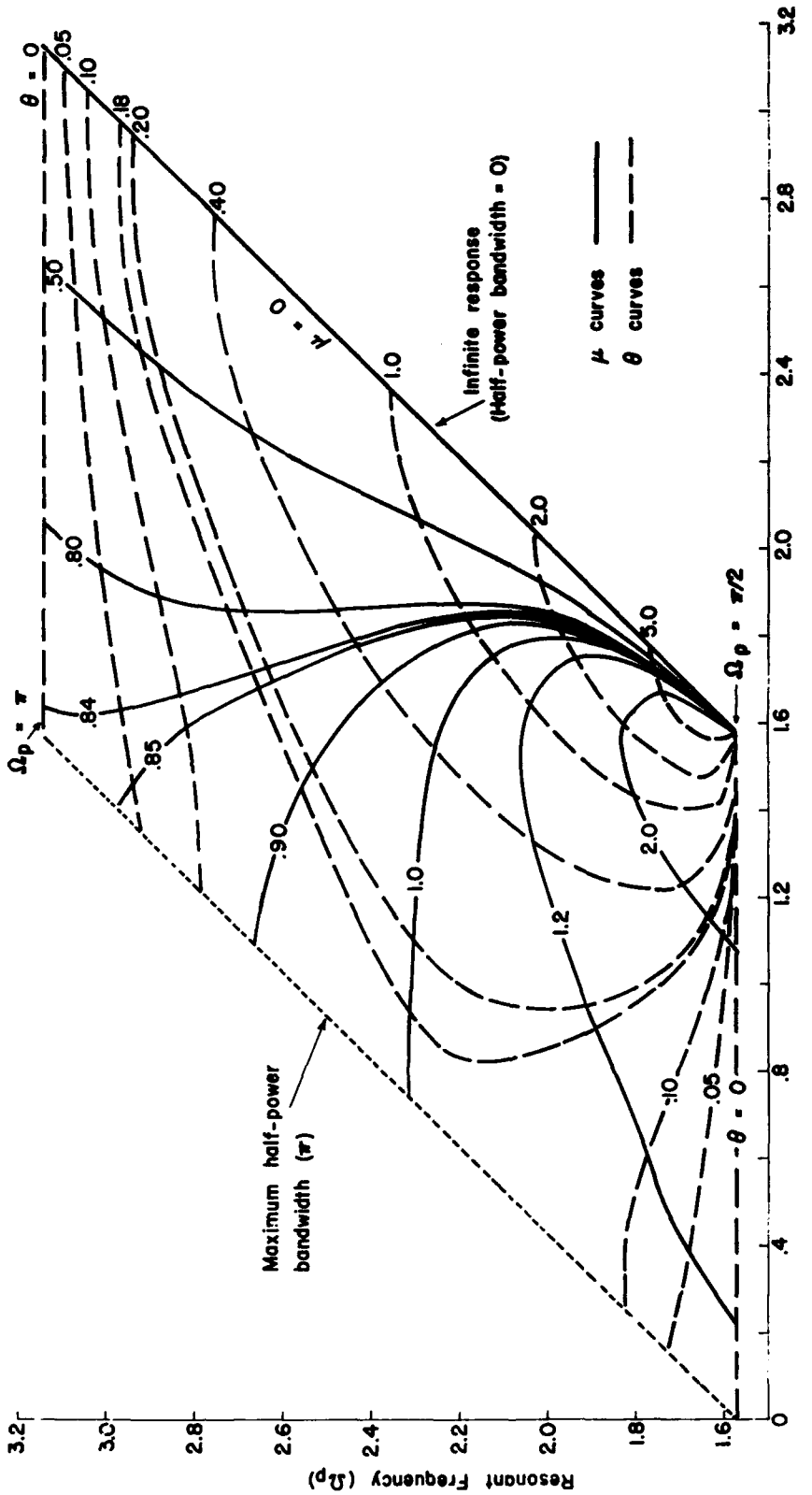

FIG. 10. Frequency at the Maximum of the Impedance at the Head End as a Function of the Frequency at the Lower Half-Power Point.

an assumption used in all the graphical results. However, this means that the distance between peaks is π always, and therefore the maximum bandwidth is also π, being $\pi/2$ on each side of a given peak.

VI. AMPLITUDE OF OSCILLATIONS ALONG THE CHAMBER; STANDING WAVE RATIO

If provision is made for measuring pressure fluctuations as a function of position along the axis, the real and imaginary parts of A_n may be determined much more readily. Equation 31 gives

$$\left|A_n + 1\right|\left|\frac{\eta}{2\eta_+}\right| = \left|e^{i\bar{\Omega}M_o z}\right|\left|\cosh\left[i\bar{\Omega}(z-1)+\phi\right]\right|$$

$$= \left|\cosh\left[\phi + i\bar{\Omega}(z-1)\right]\right|$$

$$= \sqrt{\cosh^2\alpha - \sin^2\left[\beta - \bar{\Omega}(z-1)\right]} \qquad (44)$$

where

$$\phi = \alpha + i\beta = \tanh^{-1}(-A_n) = \tanh^{-1}(-\mu - i\theta) \qquad (45)$$

This last equation can be split into real and imaginary parts:

$$\mu = -\frac{1}{4}\ln\left[\frac{(1+\alpha)^2+\beta^2}{(1-\alpha)^2+\beta^2}\right] \qquad (46)$$

$$\theta = \frac{1}{2}\tan^{-1}\left[\frac{-2\beta}{1-\alpha^2-\beta^2}\right] \qquad (47)$$

Equation 44 shows that $|\eta|$ has a maximum value (for a given frequency and η_+, or M_o') when $\beta - \bar{\Omega}(z-1) = 0, \pi, 2\pi, \ldots$, that is, when

$$\bar{\Omega}(1-z) = n\pi - \beta$$

or, in terms of the real frequency $f = \frac{\Omega}{2\pi}(1-M_c^2)\frac{a}{L}$ cps, and real distance $x = zL$,

$$\frac{2\pi f}{a(1-M_c^2)}(L-x) = n\pi - \beta$$

Thus, the first maximum occurs at a distance

$$(L - x) = (-\beta)(1 - M_c^2)\,\frac{\lambda}{2\pi} \tag{48}$$

from the exhaust if $\beta < 0$, and at a distance

$$(L - x) = (\pi - \beta)(1 - M_c^2)\,\frac{\lambda}{2\pi} \tag{49}$$

if $0 < \beta < \pi$ ($\lambda = a/f$).

Moreover, $|\eta|$ has a <u>minimum</u> value when

$$\frac{2\pi f}{a(1 - M_c^2)}\,(L - x) = (n + \tfrac{1}{2})\,\pi - \beta \tag{50}$$

i.e., at a distance

$$(L - x) = (\tfrac{\pi}{2} - \beta)(1 - M_c^2)\,\frac{\lambda}{2\pi} \tag{51}$$

from the exhaust end, if $\beta < \pi/2$, or

$$(L - x) = (\tfrac{3\pi}{2} - \beta)(1 - M_c^2)\,\frac{\lambda}{2\pi} \tag{52}$$

if $\beta < 3\pi/2$. The ratio of the maximum to minimum values of η is

$$\frac{|\eta|_{max}}{|\eta|_{min}} = \frac{\cosh \alpha}{\sqrt{\cosh^2 \alpha - 1}} = \tanh \alpha \tag{53}$$

Evidently, then, measurement of the position of a maximum or minimum of $|\eta|$ and the ratio $|\eta|_{max}/|\eta|_{min}$ is sufficient to determine α and β from Eq. 48 and 49, or 51 and 52. Finally, μ and θ can be computed from Eq. 46 and 47. An alternative approach is to use a graphical representation such as the Smith chart commonly employed in calculations for transmission lines. (See also Chapter VI of Ref. 7.) If these results are combined with measurement of the attenuation constant of freely decaying waves, then the real parts of the admittance functions for both ends of the chamber will be known.

VII. CONCLUDING REMARKS

It must be emphasized that the calculations covered in this report are intended to be coupled closely with experimental work in an effort to determine the acoustic losses associated with a rocket chamber. Although some contributions to the dissipation of energy can be computed quite accurately, such as that due to viscous shear at the walls, others which have been noted earlier, are simply beyond analysis. Moreover, the techniques discussed here can probably be extended to awkward geometries.

The principal results of the present analysis are the following:

1. The computations in section III give simple formulas for the frequency and attenuation constant for each natural mode (Eq. 17 and 18) when the influences of the ends can be lumped into simple admittance functions. This implies that the regions of transition between the uniform flow in the chamber and the end surfaces must be short compared to the chamber length; or, better, that A_n and A_o must be small.

2. The frequencies of the natural modes are not in general equal to the frequencies at which the steady-state frequency response has peaks. The former occurs at normalized values $\ell\pi - (A_o^{(r)} + \mu)$ according to Eq. 17. The latter occur when Eq. 33 has maxima. For a given mode, the two values are approximately equal when A_n is small and A_o is negligible.

3. The width of the peak in the frequency response is simply related to the transient attenuation constant only when A_n is small and A_o is negligible. If A_n is not small (i.e., the peak is broad, low Q), then the width of the peak is related to both the real and imaginary parts of A_n, but interpretation is best done graphically by making use of Fig. 2-10.

4. Measurement of the positions of maxima and minima, and the ratio of maximum to minimum ("standing wave ratio") will give the real and imaginary parts of A_n directly. If the measurements can be made without great difficulty, then this seems to be a better means of determining the losses associated with the exhaust end of the chamber.

5. The experimental results so far reported indicate that the losses, and the shift of frequency, due to the exhaust flow are very much larger than those due to the porous plate. That is, under most conditions, the porous plate seems to offer "infinite impedance." However, the validity of these results is questionable at the present time owing to some internal inconsistencies; thus the data have not been examined here.

Determination of the acoustic losses in a rocket by making measurements in a laboratory scale model, without burning, appears at the present time to be a very promising aid to design. However, the experimental work has not yet been sufficiently developed to make extensive use of the calculations discussed here.

REFERENCES

1. U. S. Naval Ordnance Test Station. Combustion of Solid Propellants and Low Frequency Combustion Instability, by Aerothermochemistry Division. China Lake, Calif., NOTS, June 1967. (NOTS TP 4244, Appendix A.)

2. Naval Weapons Center. A Comparison of Analysis and Experiment for Solid Propellant Combustion Instability, by M. W. Beckstead and F. E. C. Culick. China Lake, Calif., NWC, in preparation. (NWC TP 4531.)

3. Buffum, F. G., Jr., G. L. Dehority, R. O. Slates, and E. W. Price. "Acoustic Attenuation Experiments on Subscale, Cold-Flow Rocket Motors," AMER INST AERONAUT ASTRONAUT J, Vol. 5, No. 2 (February 1967), pp. 272-80.

4. Slates, R. O., F. G. Buffum, Jr., and G. L. Dehority. "Acoustic Attenuation in Resonant Model-Rocket Motors," in ICRPG/AIAA 2nd Solid Propulsion Conference. New York, American Institute of Aeronautics and Astronautics, 1967. Pp. 173-80.

5. Culick, F. E. C. "Acoustic Oscillations in Solid Propellant Rocket Chambers," ASTRONAUT ACTA, Vol. 12 (March-April 1966), pp. 113-26.

6. Cantrell, R. H., F. T. McClure, and R. W. Hart. "Acoustic Damping in Cavities with Mean Velocity and Thermal Boundary Layers," ACOUST SOC AMER, J, Vol. 35, No. 4 (April 1963), pp. 500-09.

7. Morse, P. M. Vibration and Sound. New York, McGraw-Hill, 1948.

INITIAL DISTRIBUTION

11 Naval Air Systems Command
- AIR-03 (1)
- AIR-03B (1)
- AIR-310 (1)
- AIR-330 (1)
- AIR-330B (1)
- AIR-503 (1)
- AIR-536 (1)
- AIR-5366 (1)
- AIR-5367 (1)
- AIR-604 (2)

4 Chief of Naval Material
- NSP-00 (1)
- NSP-001 (1)
- NSP-20 (1)
- NSP-2733 (1)

5 Naval Ordnance Systems Command
- ORD-033 (1)
- ORD-03311 (1)
- ORD-03312 (1)
- ORD-9132 (2)

1 Office of Naval Research (Code 429)

2 Naval Ordnance Laboratory, White Oak
- Carl Boyars (1)
- Technical Library (1)

2 Naval Ordnance Station, Indian Head
- L. A. Dickinson (1)
- Technical Library (1)

3 Army Missile Command, Redstone Arsenal (Redstone Scientific Information Center, Chief Document Section)

2 Army Ballistics Research Laboratories, Aberdeen Proving Ground
- Interior Ballistics Laboratory, R. C. Strittmater (1)
- Technical Library (1)

2 Picatinny Arsenal
- J. Picard (1)
- Technical Library (1)

1 Sunflower Army Ammunition Plant (SMUSU-R)

1 Air Force Office of Scientific Research (Propulsion Division, Dr. Bernard T. Wolfson)

2 Air Force Rocket Propulsion Laboratory, Edwards (RPMCP)
  Capt. C. E. Payne (1)
  Richard Spann (1)
2 6593 Test Group, Edwards Air Force Base (Development, Don Hart)
1 Advanced Research Projects Agency (Technical Information Office)
20 Defense Documentation Center
1 Bureau of Mines, Pittsburgh (Explosive Research Center, I. Liebman)
19 National Aeronautics and Space Administration
  MGS, E. Hall (1)
  MTA, M. C. Waugh (1)
  NaPO, John J. Stashak (1)
  RC, J. L. Sloop (1)
  RF, R. D. Ginter (1)
  RP, A. O. Tischler (1)
  RPM, William Cohen (1)
  RPS, R. Ziem (5)
  RTA, R. V. Hensley (1)
  RTP, J. J. Phillips (1)
  RV, M. B. Ames (1)
  RV-1, R. W. May, Jr. (1)
  SV, V. L. Johnson (1)
  ATSS-AC, Technical Library (2)
1 George C. Marshall Space Flight Center (Technical Library)
1 Goddard Space Flight Center (Technical Library)
2 Langley Research Center
  Robert L. Swain (1)
  Technical Library (1)
4 Lewis Research Center
  Dr. Louis A. Povinelli (1)
  Dr. Richard J. Priem (1)
  James J. Kramer (1)
  Technical Library (1)
2 Manned Spacecraft Center
  J. G. Thibodaux (1)
  Technical Library (1)
1 NASA Scientific and Technical Information Facility, College Park, Md. (CRT)
1 Aerojet-General Corporation, Azusa, Calif. (Library), via NPRO
3 Aerojet-General Corporation, Sacramento, via AFPRO
  J. Wiegand (1)
  Department 4730 (1)
  Head, Technical Information Office (1)
1 Aerospace Corporation, Los Angeles (Library)
2 Allegany Ballistics Laboratory, Cumberland, Md.
  T. A. Angelus (1)
  Technical Library (1)
2 Applied Physics Laboratory, JHU, Silver Spring
  Dr. W. H. Avery (1)
  Dr. Robert H. Cantrell (1)

3 Atlantic Research Corporation, Alexandria, Va.
  Dr. Raymond Friedman (1)
  K. Woodcock (1)
  Technical Library (1)
1 Bermite Powder Company, Saugus, Calif.
1 Bolt, Beranek and Newman, Inc., Cambridge, Mass. (E. E. Unger)
1 Brigham Young University, Provo, Utah (R. L. Coates)
1 Bruce H. Sage Consultant, Pasadena
2 California Institute of Technology, Pasadena
  Dr. F. E. C. Culick (1)
  Dr. Frank E. Marble (1)
1 CETEC Corporation, Mountain View, Calif. (R. Anderson)
2 Chemical Propulsion Information Agency, Applied Physics Laboratory, Silver Spring
  T. W. Christian, III (1)
  Technical Library (1)
1 Columbia University, New York (Department of Mechanical Engineering, Dr. R. A. Gross)
1 Cornell Aeronautical Laboratory, Inc., Buffalo (Dr. G. H. Markstein)
1 Davidson Laboratory, Stevens Institute of Technology, Hoboken, N. J. (R. F. McAlvey, III)
1 Defense Research Corporation, Santa Barbara (Dr. A. Berlad)
1 Georgia Institute of Technology, Atlanta (Dr. B. Zinn)
1 Hercules Incorporated, Bacchus, Utah (Technical Library)
1 Institute for Defense Analyses, Arlington (Technical Library)
3 Jet Propulsion Laboratory, CIT, Pasadena
  Dr. Leon Strand (1)
  Winston Gin (1)
  Technical Library (1)
1 Lockheed Missiles and Space Company, Palo Alto (C. A. Zimmerman)
2 Lockheed Propulsion Company, Redlands, Calif.
  Dr. M. W. Beckstead (1)
  Technical Library (1)
1 Marquardt Corporation, Van Nuys, Calif. (Technical Library)
1 Martin Company, Denver (R. Knoll)
1 Northern Research and Engineering Corporation, Cambridge, Mass. (K. Bastress)
1 Pennsylvania State University, University Park (Mechanical Engineering Department, G. M. Faeth)
2 Princeton University, Forrestal Campus Library
  Dr. Irvin Glassman (1)
  Dr. Martin Summerfield (1)
1 Purdue University, Lafayette, Ind. (School of Mechanical Engineering, Dr. John R. Osborn)
1 Rocket Research Corporation, Seattle (Technical Library)
3 Rocketdyne, Canoga Park, Calif.
  Dr. G. Lo (1)
  C. L. West (1)
  Library, Department 596-306 (1)

UNCLASSIFIED
Security Classification

DOCUMENT CONTROL DATA - R&D

(Security classification of title, body of abstract and indexing annotation must be entered when the overall report is classified)

1. ORIGINATING ACTIVITY *(Corporate author)*
Naval Weapons Center
China Lake, California 93555

2a. REPORT SECURITY CLASSIFICATION
UNCLASSIFIED

2b. GROUP

3. REPORT TITLE
AN ANALYSIS OF AXIAL ACOUSTIC WAVES IN A COLD-FLOW ROCKET

4. DESCRIPTIVE NOTES *(Type of report and inclusive dates)*
Research Report

5. AUTHOR(S) *(Last name, first name, initial)*
Culick, F. E. C.; Dehority, G. L.

6. REPORT DATE	7a. TOTAL NO. OF PAGES	7b. NO. OF REFS
May 1968	32	7

8a. CONTRACT OR GRANT NO.	9a. ORIGINATOR'S REPORT NUMBER(S)
b. PROJECT NO.	NWC TP 4544
c. TA ORD-033 103/200 1/F009-06-01, PA #3	9b. OTHER REPORT NO(S) *(Any other numbers that may be assigned this report)*
d.	

10. AVAILABILITY/LIMITATION NOTICES
This document is subject to special export controls and each transmittal to foreign governments or foreign nationals may be made only with prior approval of the Naval Weapons Center.

11. SUPPLEMENTARY NOTES	12. SPONSORING MILITARY ACTIVITY
	Naval Ordnance Systems Command Naval Materials Command Washington, D. C. 20360

13. ABSTRACT

The presence of waves in a rocket chamber depends on the relative importance of energy supplied by interaction with the combustion processes and energy lost through dissipative processes. As an aid to assessing the latter, the cold-flow rocket appears to be a promising tool for both research and development. Combustion is absent and acoustic waves are excited mechanically in a chamber through which a steady flow is maintained. The analysis presented here is intended to serve as a basis for interpreting such measurements. Only the case of axial, or longitudinal waves is treated, and results show mainly how the losses at the exhaust end of the chamber may be inferred from measurements of the transient response and the frequency response of a chamber.

DD FORM 1 JAN 64 1473 0101-807-6800

UNCLASSIFIED
Security Classification

14. KEY WORDS	LINK A		LINK B		LINK C	
	ROLE	WT	ROLE	WT	ROLE	WT
Instability Acoustic damping Nozzle damping Cold-flow						

INSTRUCTIONS

1. ORIGINATING ACTIVITY: Enter the name and address of the contractor, subcontractor, grantee, Department of Defense activity or other organization *(corporate author)* issuing the report.

2a. REPORT SECURITY CLASSIFICATION: Enter the overall security classification of the report. Indicate whether "Restricted Data" is included. Marking is to be in accordance with appropriate security regulations.

2b. GROUP: Automatic downgrading is specified in DoD Directive 5200.10 and Armed Forces Industrial Manual. Enter the group number. Also, when applicable, show that optional markings have been used for Group 3 and Group 4 as authorized.

3. REPORT TITLE: Enter the complete report title in all capital letters. Titles in all cases should be unclassified. If a meaningful title cannot be selected without classification, show title classification in all capitals in parenthesis immediately following the title.

4. DESCRIPTIVE NOTES: If appropriate, enter the type of report, e.g., interim, progress, summary, annual, or final. Give the inclusive dates when a specific reporting period is covered.

5. AUTHOR(S): Enter the name(s) of author(s) as shown on or in the report. Enter last name, first name, middle initial. If military, show rank and branch of service. The name of the principal author is an absolute minimum requirement.

6. REPORT DATE: Enter the date of the report as day, month, year; or month, year. If more than one date appears on the report, use date of publication.

7a. TOTAL NUMBER OF PAGES: The total page count should follow normal pagination procedures, i.e., enter the number of pages containing information.

7b. NUMBER OF REFERENCES: Enter the total number of references cited in the report.

8a. CONTRACT OR GRANT NUMBER: If appropriate, enter the applicable number of the contract or grant under which the report was written.

8b, 8c, & 8d. PROJECT NUMBER: Enter the appropriate military department identification, such as project number, subproject number, system numbers, task number, etc.

9a. ORIGINATOR'S REPORT NUMBER(S): Enter the official report number by which the document will be identified and controlled by the originating activity. This number must be unique to this report.

9b. OTHER REPORT NUMBER(S): If the report has been assigned any other report numbers *(either by the originator or by the sponsor)*, also enter this number(s).

10. AVAILABILITY/LIMITATION NOTICES: Enter any limitations on further dissemination of the report, other than those imposed by security classification, using standard statements such as:

(1) "Qualified requesters may obtain copies of this report from DDC."

(2) "Foreign announcement and dissemination of this report by DDC is not authorized."

(3) "U. S. Government agencies may obtain copies of this report directly from DDC. Other qualified DDC users shall request through _____."

(4) "U. S. military agencies may obtain copies of this report directly from DDC. Other qualified users shall request through _____."

(5) "All distribution of this report is controlled. Qualified DDC users shall request through _____."

If the report has been furnished to the Office of Technical Services, Department of Commerce, for sale to the public, indicate this fact and enter the price, if known.

11. SUPPLEMENTARY NOTES: Use for additional explanatory notes.

12. SPONSORING MILITARY ACTIVITY: Enter the name of the departmental project office or laboratory sponsoring *(paying for)* the research and development. Include address.

13. ABSTRACT: Enter an abstract giving a brief and factual summary of the document indicative of the report, even though it may also appear elsewhere in the body of the technical report. If additional space is required, a continuation sheet shall be attached.

It is highly desirable that the abstract of classified reports be unclassified. Each paragraph of the abstract shall end with an indication of the military security classification of the information in the paragraph, represented as *(TS), (S), (C), or (U)*.

There is no limitation on the length of the abstract. However, the suggested length is from 150 to 225 words.

14. KEY WORDS: Key words are technically meaningful terms or short phrases that characterize a report and may be used as index entries for cataloging the report. Key words must be selected so that no security classification is required. Identifiers, such as equipment model designation, trade name, military project code name, geographic location, may be used as key words but will be followed by an indication of technical context. The assignment of links, roles, and weights is optional.

ABSTRACT CARD

Naval Weapons Center
An Analysis of Axial Acoustic Waves in a Cold-Flow Rocket, by F. E. C. Culick and G. L. Dehority. China Lake, Calif., NWC, May 1968. 32 pp. (NWC TP 4544), UNCLASSIFIED.

ABSTRACT. The presence of waves in a rocket chamber depends on the relative importance of energy supplied by interaction with the combustion processes and energy lost through dissipative processes. As an aid to assessing the latter, the cold-flow rocket

(Over)
1 card, 8 copies

Naval Weapons Center
An Analysis of Axial Acoustic Waves in a Cold-Flow Rocket, by F. E. C. Culick and G. L. Dehority. China Lake, Calif., NWC, May 1968. 32 pp. (NWC TP 4544), UNCLASSIFIED.

ABSTRACT. The presence of waves in a rocket chamber depends on the relative importance of energy supplied by interaction with the combustion processes and energy lost through dissipative processes. As an aid to assessing the latter, the cold-flow rocket

(Over)
1 card, 8 copies

Naval Weapons Center
An Analysis of Axial Acoustic Waves in a Cold-Flow Rocket, by F. E. C. Culick and G. L. Dehority. China Lake, Calif., NWC, May 1968. 32 pp. (NWC TP 4544), UNCLASSIFIED.

ABSTRACT. The presence of waves in a rocket chamber depends on the relative importance of energy supplied by interaction with the combustion processes and energy lost through dissipative processes. As an aid to assessing the latter, the cold-flow rocket

(Over)
1 card, 8 copies

Naval Weapons Center
An Analysis of Axial Acoustic Waves in a Cold-Flow Rocket, by F. E. C. Culick and G. L. Dehority. China Lake, Calif., NWC, May 1968. 32 pp. (NWC TP 4544), UNCLASSIFIED.

ABSTRACT. The presence of waves in a rocket chamber depends on the relative importance of energy supplied by interaction with the combustion processes and energy lost through dissipative processes. As an aid to assessing the latter, the cold-flow rocket

(Over)
1 card, 8 copies

appears to be a promising tool for both research and development. Combustion is absent and acoustic waves are excited mechanically in a chamber through which a steady flow is maintained. The analysis presented here is intended to serve as a basis for interpreting such measurements. Only the case of axial, or longitudinal waves is treated, and results show mainly how the losses at the exhaust end of the chamber may be inferred from measurements of the transient response and the frequency response of a chamber.

NWC TP 4544

appears to be a promising tool for both research and development. Combustion is absent and acoustic waves are excited mechanically in a chamber through which a steady flow is maintained. The analysis presented here is intended to serve as a basis for interpreting such measurements. Only the case of axial, or longitudinal waves is treated, and results show mainly how the losses at the exhaust end of the chamber may be inferred from measurements of the transient response and the frequency response of a chamber.

NWC TP 4544

appears to be a promising tool for both research and development. Combustion is absent and acoustic waves are excited mechanically in a chamber through which a steady flow is maintained. The analysis presented here is intended to serve as a basis for interpreting such measurements. Only the case of axial, or longitudinal waves is treated, and results show mainly how the losses at the exhaust end of the chamber may be inferred from measurements of the transient response and the frequency response of a chamber.

NWC TP 4544

appears to be a promising tool for both research and development. Combustion is absent and acoustic waves are excited mechanically in a chamber through which a steady flow is maintained. The analysis presented here is intended to serve as a basis for interpreting such measurements. Only the case of axial, or longitudinal waves is treated, and results show mainly how the losses at the exhaust end of the chamber may be inferred from measurements of the transient response and the frequency response of a chamber.

ABSTRACT CARD

Naval Weapons Center
An Analysis of Axial Acoustic Waves in a Cold-Flow Rocket, by F. E. C. Culick and G. L. Dehority. China Lake, Calif., NWC, May 1968. 32 pp. (NWC TP 4544), UNCLASSIFIED.

ABSTRACT. The presence of waves in a rocket chamber depends on the relative importance of energy supplied by interaction with the combustion processes and energy lost through dissipative processes. As an aid to assessing the latter, the cold-flow rocket

(Over)
1 card, 8 copies

Naval Weapons Center
An Analysis of Axial Acoustic Waves in a Cold-Flow Rocket, by F. E. C. Culick and G. L. Dehority. China Lake, Calif., NWC, May 1968. 32 pp. (NWC TP 4544), UNCLASSIFIED.

ABSTRACT. The presence of waves in a rocket chamber depends on the relative importance of energy supplied by interaction with the combustion processes and energy lost through dissipative processes. As an aid to assessing the latter, the cold-flow rocket

(Over)
1 card, 8 copies

Naval Weapons Center
An Analysis of Axial Acoustic Waves in a Cold-Flow Rocket, by F. E. C. Culick and G. L. Dehority. China Lake, Calif., NWC, May 1968. 32 pp. (NWC TP 4544), UNCLASSIFIED.

ABSTRACT. The presence of waves in a rocket chamber depends on the relative importance of energy supplied by interaction with the combustion processes and energy lost through dissipative processes. As an aid to assessing the latter, the cold-flow rocket

(Over)
1 card, 8 copies

Naval Weapons Center
An Analysis of Axial Acoustic Waves in a Cold-Flow Rocket, by F. E. C. Culick and G. L. Dehority. China Lake, Calif., NWC, May 1968. 32 pp. (NWC TP 4544), UNCLASSIFIED.

ABSTRACT. The presence of waves in a rocket chamber depends on the relative importance of energy supplied by interaction with the combustion processes and energy lost through dissipative processes. As an aid to assessing the latter, the cold-flow rocket

(Over)
1 card, 8 copies

appears to be a promising tool for both research and development. Combustion is absent and acoustic waves are excited mechanically in a chamber through which a steady flow is maintained. The analysis presented here is intended to serve as a basis for interpreting such measurements. Only the case of axial, or longitudinal waves is treated, and results show mainly how the losses at the exhaust end of the chamber may be inferred from measurements of the transient response and the frequency response of a chamber.

NWC TP 4544

appears to be a promising tool for both research and development. Combustion is absent and acoustic waves are excited mechanically in a chamber through which a steady flow is maintained. The analysis presented here is intended to serve as a basis for interpreting such measurements. Only the case of axial, or longitudinal waves is treated, and results show mainly how the losses at the exhaust end of the chamber may be inferred from measurements of the transient response and the frequency response of a chamber.

NWC TP 4544

appears to be a promising tool for both research and development. Combustion is absent and acoustic waves are excited mechanically in a chamber through which a steady flow is maintained. The analysis presented here is intended to serve as a basis for interpreting such measurements. Only the case of axial, or longitudinal waves is treated, and results show mainly how the losses at the exhaust end of the chamber may be inferred from measurements of the transient response and the frequency response of a chamber.

NWC TP 4544

appears to be a promising tool for both research and development. Combustion is absent and acoustic waves are excited mechanically in a chamber through which a steady flow is maintained. The analysis presented here is intended to serve as a basis for interpreting such measurements. Only the case of axial, or longitudinal waves is treated, and results show mainly how the losses at the exhaust end of the chamber may be inferred from measurements of the transient response and the frequency response of a chamber.

2 Rocketdyne, McGregor, Tex.
S. C. Britton (1)
Technical Library (1)
2 Rohm and Haas Company, Redstone Arsenal Research Division
Dr. William A. Wood (1)
Technical Library (1)
1 Sandia Corporation, Albuquerque (Dr. Lloyd S. Nelson)
2 Stanford Research Institute, Menlo Park, Calif.
Dr. M. Evans (1)
Dr. G. A. Marxman (1)
1 Texaco Experiment, Inc., Richmond, Va. (U. V. Henderson)
2 Thiokol Chemical Corporation, Elkton, Md.
E. E. Hackman (1)
Technical Library (1)
2 Thiokol Chemical Corporation, Huntsville Division, Huntsville, Ala.
Technical Director (1)
D. A. Flanigan (1)
2 Thiokol Chemical Corporation, Wasatch Division, Brigham City
Dr. R. Reed, Jr. (1)
Technical Library (1)
1 United Aircraft Corporation, East Hartford (Research Laboratories, Dr. R. Waesche)
3 United Technology Center, Sunnyvale, Calif.
Dr. R. S. Brown (1)
Dr. Robert W. Hermsen (1)
Technical Library (1)
2 University of California, Berkeley
Aeronautical Science Division, Dr. A. K. Oppenheim (1)
Chemistry Department, E. Peterson (1)
2 University of California, San Diego, La Jolla (Department of Aerospace Engineering)
Dr. Stanford S. Penner (1)
F. A. Williams (1)
1 University of Denver, Denver Research Institute (James Kottenstette)
2 University of Utah, Salt Lake City (Department of Chemical Engineering)
Prof. A. Baer (1)
Prof. N. W. Ryan (1)